

# A Functional Coefficients Version of a Generalized Orr–Sherby–Dorn Creep Model: An Application to 2.25Cr–1Mo Steel



M. EVANS

It is important to be able to predict the creep life of materials used in power plants. This paper illustrates the inadequacies of the Orr–Sherby–Dorn (OSD) creep model in achieving this aim for 2.25Cr–1Mo steel. This failure is explained in terms of non-constant model parameters—which in turn is the result of changing creep mechanisms. The paper introduces a semi-parametric estimation procedure for a variant of the OSD model (a structural coefficients version) that can be used to deal with such changing creep mechanisms while maintaining the structure of the model and consequently producing more reliable long-term predictions compared to the unmodified OSD model and the recently introduced LOESS technique. For 2.25Cr–1Mo steel, it was found that the model parameters varied in line with changing creep mechanisms, but in a modified way compared to that already suggested in the literature for this material. The models used suggested that with diminishing stress and increasing temperature, dislocation creep within the crystal structure morphs into grain boundary dislocation motion and finally Nabarro–Herring creep.

<https://doi.org/10.1007/s11661-024-07437-1>  
© The Author(s) 2024

## I. INTRODUCTION

FOR materials operating at high temperatures, the understanding of creep and its interaction with other damage mechanism such as fatigue and oxidation is of great importance. Indeed, creep is the dominant failure mechanism for pipework that is used to transport steam from boilers to turbines in power plants. 2.25Cr–1Mo is a main stay steel used for such structural components within the UK’s aging power plants—where the usual service conditions for heater tubes is around 840 K and 35 MPa. Under these static conditions, this material is designed to resist creep failure up to 250,000 h of operation. The development of new materials that can operate at higher temperatures, to improve efficiency levels, is however considerably hampered by the fact that currently there are few creep models that have proved capable of accurately extrapolating accelerated test data (out only to around 5000–10,000 h) to such operating conditions.<sup>[1]</sup> Studies on low alloyed steels typically reveal substantial downward revisions in

estimated creep life as longer-term test results become available over time.

Many of the traditional parametric creep models such as the Larson–Miller,<sup>[2]</sup> Manson–Haferd,<sup>[3]</sup> and the Dorn and Shepherd<sup>[4]</sup> models have as their basis the simple Arrhenius expression for relating minimum creep rates to temperature. The Dorn–Shepherd model is usually written in terms of the minimum creep rate  $\dot{\epsilon}_m$ , but using the Monkman–Grant<sup>[5]</sup> relation with an exponent of unity, it can also be written in terms of time to failure  $t_F$

$$t_F = \frac{M}{\dot{\epsilon}_m} = D\sigma^{(-n)} \exp\left(\frac{Q_c}{RT}\right), \quad [1a]$$

where  $\sigma$  is stress,  $T$  is absolute temperature, and  $M$ ,  $n$  (sometimes termed Norton’s  $n$ ), and  $D$  are unknown model constants.  $Q_c$  is the activation energy for creep. This can be linearized using natural logs

$$\ln(t_F) = \left\{ \ln(D) + Q_c \left( \frac{1}{RT} \right) \right\} - n \ln(\sigma), \quad [1b]$$

so that at constant temperature the model predicts a linear (and negative) relationship between  $\ln(t_F)$  and  $\ln(\sigma)$  with the effect of temperature then being to shift this linear relationship in a parallel fashion (i.e., change only the intercept  $D$  in the model). When this model is applied to minimum creep rates obtained by the Japanese National Institute for Materials Science

M. EVANS is with the Institute of Structural Materials, Swansea University Bay Campus, Swansea, SA1 8EN Wales. Contact e-mail: [m.evans@swansea.ac.uk](mailto:m.evans@swansea.ac.uk)  
Manuscript submitted November 23, 2023; accepted May 5, 2024.

(NIMS)<sup>[6,7]</sup> on one batch (termed MAF) of 2.25Cr–1Mo steel, the results seen in Figure 1(a) are obtained. Figure 1(a) plots various isothermal lines and it can be seen that Norton's  $n$  [the power of  $x$  in Figure 1(a)] is not a model constant. Clearly,  $n$  tends to diminish with increasing temperature.

Figure 1(b) plots various iso-stress lines, and the activation energy for creep is also far from a constant—tending to diminish with increasing temperature. But again, is not clear if this is just a temperature dependency as the lower  $Q_c$  value [of  $325 \text{ kJ mol}^{-1}$ —the power of  $e$  in Figure 1(b)] also occurs at the lowest stress. It is this variation in  $n$  and  $Q_c$  that leads to the OSD model producing unreliable long-term predictions based on shorter-term data.

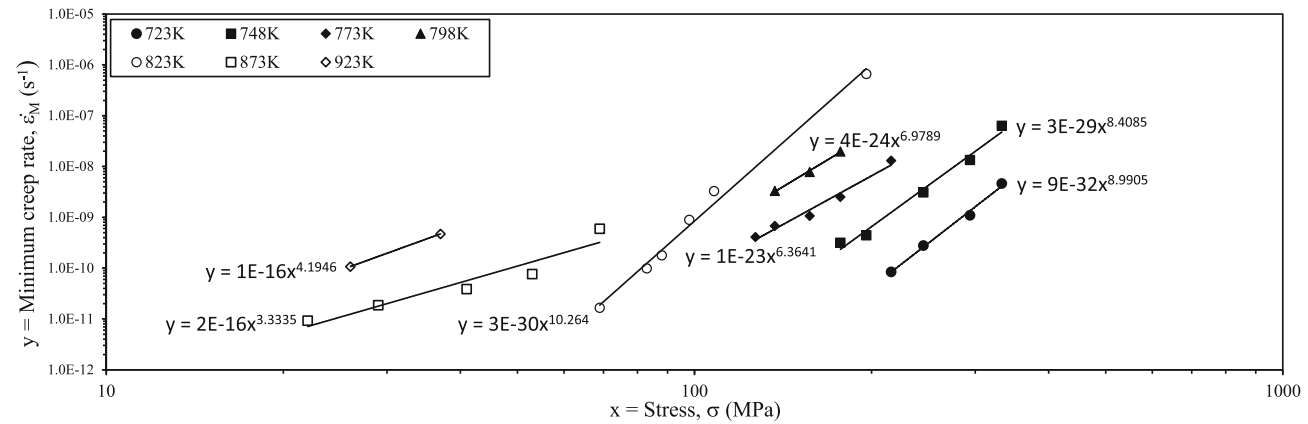
There is a tendency in the literature to attribute these changes in  $n$  and  $Q_c$  values to different creep mechanisms applying over different stress and temperature ranges. Some solutions to this problem of changing creep mechanisms are present in the literature. A recent approach taken by Ding *et al.*<sup>[8]</sup> is to specify a separate equation to explain creep rates due to grain boundary sliding, dislocation creep, and dislocation glide. The overall creep rate is then simply the sum of the creep rates predicted by these mechanisms. Integration using true stress and true strain then yields an expression for

predicting the observed creep curve at any point in time based on these evolving creep mechanisms. The approach is readily extended to encompass other mechanisms—for example to include a role for high-temperature oxidation. By modeling the whole creep curve, this approach can predict the role of both primary creep and microstructure evolution on time to failure.

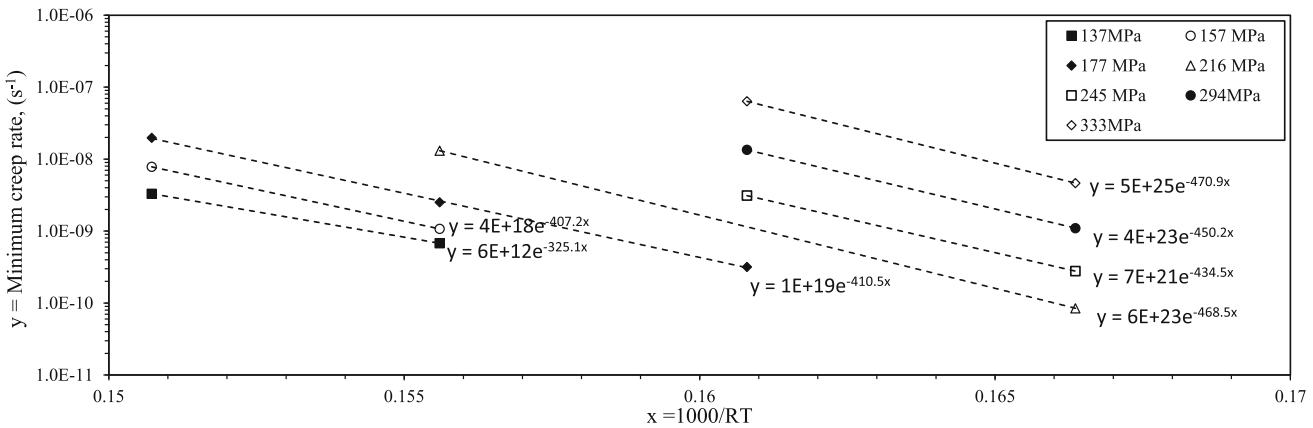
This paper makes use of varying parameter models common in the statistical literature to deal with the non-constancy of  $n$  and  $Q_c$ . Recently, Evans<sup>[9]</sup> made a first attempt at this by proposing a semi-parametric approach based on the LOESS technique. Here, the parametric form of a particular creep model corresponding to a fixed temperature is estimated by least squares or weighted least squares. For example, the OSD model at constant temperature has the form

$$\ln(t_F) = a - n \ln(\sigma), \quad [1c]$$

where  $a = \ln(D) + Q_c \left( \frac{1}{RT} \right)$  is a constant if  $T$  is held fixed. LOESS then involves selecting one of the test stresses ( $\sigma_0$ ) in the test matrix and applying least squares or weighted least squares to estimate  $a$  and  $b$ , but instead of using all test results, only the nearest ones to  $\sigma_0$  are used. This is then repeated for all values of  $\sigma_0$  in the test matrix and so what emerges from such repetition are



(a)



(b)

Fig. 1—The variation in minimum creep rates shown in NIMS creep data sheets 3B & 50A<sup>[6,7]</sup> with (a) stress at constant temperature and (b) reciprocal of temperature at constant stress.

values for  $a$  and  $b$  that can be associated with each stress. By applying this OSD model over such a local range of stresses, the creep mechanism remains approximately constant, so allowing for more accurate creep life predictions. This LOESS model was shown by Evans<sup>[9]</sup> to produce better extrapolations of creep life than a fully parametric OSD model.

However, this approach comes with several limitations and complications. First, the functional relationships between the parameters  $a$  and  $b$  and stress can only be identified by plotting  $a$  and  $n$  against stress, and then as a second stage, fitting trend lines to such plots. From a statistical perspective, such a two-stage estimation procedure produces less efficient estimates of the parameters of this trend line than any potential one-step procedure. By less efficient it is meant the parameters are not estimated with the smallest possible variance or level of sample variation uncertainty. Furthermore, the approach says nothing about the correct functional form of this trend line, which is currently unknown.

Secondly, LOESS only works for models containing one explanatory variable, but time to failure also depends on temperature. Evans<sup>[9]</sup> incorporated temperature into this LOESS model by introducing sub repetitions within the above-described repetitive process. But this came at cost. A relatively minor issue is that it results in a rather computer intensive estimation procedure that some readers and practitioner's dislike. For example, Evans<sup>[9]</sup> incorporated  $T$  into the OSD model using a temperature compensated failure time

$$\ln(t_F) - \frac{Q_c}{RT} = a - n \ln(\sigma), \quad [1d]$$

where now  $a = \ln(D)$ . LOESS then involves guessing a value for the activation energy  $Q_c$ , selecting one of the test stresses ( $\sigma_0$ ) in the test matrix and applying least squares or weighted least squares to estimate  $a$  and  $b$ , using nearest test results to  $\sigma_0$ . This is then repeated for all values of  $\sigma_0$  in the test matrix and so what emerges from such repetition are values for  $a$  and  $b$  that can be associated with each stress. Finally,  $Q_c$  is varied in a structured way until the fit to the temperature-adjusted failure times is maximized.

While Evans<sup>[9]</sup> showed that temperature adjusting stress as well as times opens up the LOESS procedure to other well-known creep models such as the Soviet model<sup>[10]</sup> and the Minimum Commitment Methods<sup>[11]</sup>, it forces the activation energy to be a constant that does not vary with stress. Yet, changing creep mechanisms will often be associated with a change in activation energy, and Evans<sup>[9]</sup> stated that this limitation warranted future research to relax the constraint of a constant  $Q_c$ . This paper presents the functional coefficient model as a solution to this identified shortcoming of LOESS. Closely related to the above point is the fact that each local regression in the above LOESS procedure is over a local range of stresses and not temperatures. But creep mechanisms also vary with temperature and the local regressions may therefore not be over constant creep mechanism conditions. So, it may be possible to improve life predictions by defining

local in terms of stress and temperature, i.e., by local test conditions and not just local stress.

The first issue mentioned above (an unknown functional relationship between  $n$  and  $Q_c$  with both stress and temperature) can be dealt with by approximating these unknown functions with a Taylor series expansion. This can be of any order, but this paper restricts itself to first and second-order Taylor series approximations. The second problem can be dealt by (i) including  $T$  as an additional explanatory variable on the right-hand side of Eq. [1c] and (ii) defining close in a local regression as similar stress-temperature combinations to the one under investigation. This allows  $Q_c$  to vary with stress and temperature and allows estimation of all the models unknown parameters to be done in a single stage or step. The result is a functional coefficients model<sup>[12]</sup>.

Therefore, the aim of this paper is to implement the suggestion made by Evans<sup>[9]</sup> of developing a fully variable parameter model (allowing  $Q_c$  to vary as well) to predict creep failure times. This is done by introducing readers to the functional coefficients model that overcomes the limitations of the LOESS procedure proposed by Evans. The second aim is to assess whether this model is still capable of producing predictions of time to failure that are *i.* at least comparable with that produced by LOESS and *ii.* superior to a fully parametric creep model. The third aim of the paper is to try and explain the pattern of the varying creep model parameters that the functional coefficients model produces, in terms of changing creep mechanisms. To achieve these aims, experimental failure time data on 2.25Cr-1Mo steel produced by NIMS<sup>[6,7]</sup> will be used. The next section therefore describes these NIMS data. This is followed by a method section that outlines the structure of a functional coefficient model to reveal its inherent flexibility in creep model specification compared to the LOESS technique. A section on how the unknown parameters of such a model are estimated then follows. The penultimate results section then compares the functional coefficients models to a fully parametric OSD model and a LOESS version of this model. Finally, conclusions are drawn.

## II. THE DATA

This paper makes use of the information in Creep Data Sheets 3B, 50A, published by the Japanese National Institute for Materials Science (NIMS).<sup>[6,7]</sup> These have extensive data on twelve batches of 2.25Cr-1Mo (according to ASTM A 387, Grade 22) steel where each batch has a different chemical composition that underwent one of four different heat treatments—details of which are given in Reference 6. This paper makes use of just one of these batches, the MAF batch, which was in tube form that had an outside diameter of 50.8 mm, a wall thickness of 8 mm, and a length of 5000 mm with a chemical composition of Fe-2.46 Cr-0.94Mo-0.1C-0.23Si-0.43Mn-0.011P-0.009S-0.008Ni-0.07Cu-0.005Al. Specimens for creep testing were taken longitudinally from this material. Each test specimen had a diameter of 6 mm with a gauge length of 30 mm. The creep tests were obtained over a wide range of conditions:

400–22 MPa and 723–923 K. For the MAF batch (and only this batch), both minimum creep rates and time to failure measurements were recorded, together with the times to attain various strains – 0.005, 0.01, 0.02, and 0.05. Figure 2 plots the creep failure times obtained for this MAF batch at the different stresses and temperatures used.

### III. METHOD

#### A. Fully Parametric Creep Models

The Orr–Sherby–Dorn (OSD) and Larson–Miller (LM) models have as their basis the Arrhenius relation, that when applied to creep explains the relationship between absolute temperature and the minimum creep rate at a constant load or stress. The Arrhenius expression is typically used to relate the minimum creep rate to temperature but combining it with the Monkman–Grant relation also allows it to also be written in terms of the time to failure

$$\dot{\epsilon}_m = A \exp\left(-\frac{Q_c}{RT}\right) = \frac{M}{t_F}, \quad [2a]$$

$$t_F = \frac{M}{A} \exp\left(\frac{Q_c}{RT}\right). \quad [2b]$$

The OSD model has as its foundation this Arrhenius relation and introduces the effect of stress on the time to failure by making the parameter  $M/A$  a function of stress. More specifically, the OSD model postulates that

$$\ln(t_F) = \left\{ \ln(D) + Q_c \left( \frac{1}{RT} \right) \right\} - n \ln(\sigma), \quad [2c]$$

$M/A = f_{\text{OSD}}(\sigma) = D\sigma^{-n}$ , so that

Consequently, in the OSD model, the effect of temperature is to shift in a parallel fashion the isothermal lines when plotted in  $\ln(t_F)$ – $\ln(\sigma)$  space. As temperature changes by  $\Delta T$ , the slope of the isothermal line remains unchanged at the value given by  $n$  in Eq. [2c], but its intercept changes by  $Q_c \left( \frac{1}{R} \Delta T \right)$ . If  $\sigma$  is replaced with  $\ln(\ln(\sigma_{\text{TS}}/\sigma))$  in Eq. [2c], the Wilshire<sup>[13]</sup> creep model emerges (where  $\sigma_{\text{TS}}$  is the materials tensile strength).

The LM model also has as its foundation the Arrhenius relation, but in this model it is parameter  $Q_c$  that is made a function of stress  $Q_c = f_{\text{LM}}(\sigma)$ . This functional relationship is postulated differently in different applications of the LM model, but a typical specification is  $Q_c = B_0 + B_1 \ln(\sigma)$ , where the  $B$  are further model parameters. Substituting this into Eq. [2c] gives one representation of the LM model

$$\ln(t_F) = \ln(M/A) + B_0 \left( \frac{1}{RT} \right) + B_1 \left( \frac{\ln(\sigma)}{RT} \right). \quad [2d]$$

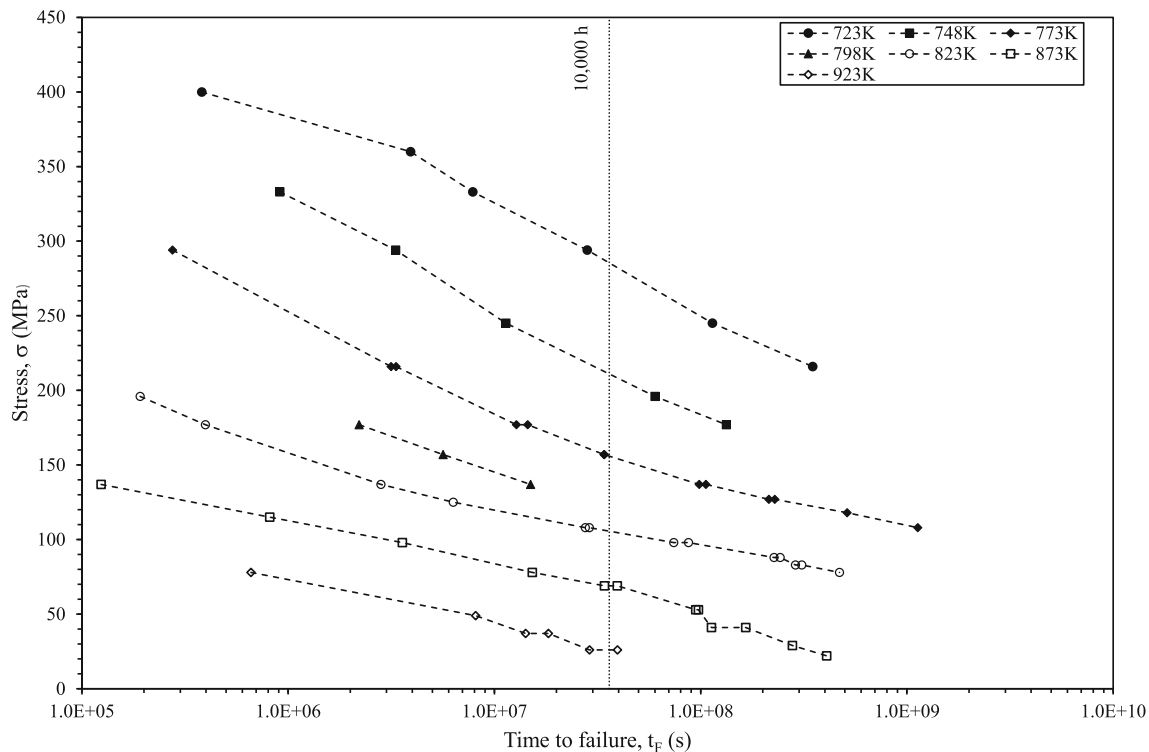


Fig. 2—Relationship between stress, temperature, and time to failure for the MAF batch of 2.25Cr–1Mo steel contained within NIMS creep data sheets 3B & 50A.<sup>[6,7]</sup>

Consequently, in the LM model, the effect of temperature is to shift and rotate the isothermal lines when plotted in  $\ln(t_F)$ – $\ln(\sigma)$  space. The LM model predicts that the slope of the isothermal lines should be given by  $\left(\frac{B}{RT}\right)$  and so changes with temperature. The LM model also predicts that the intercept of the isothermal lines is given by  $\ln(M/A) + B_0\left(\frac{1}{RT}\right)$  and so also changes with temperature.

The changing intercept of the isothermal lines shown in Figure 1(a) with changes in temperature is consistent with the OSD model, but the reduction in Norton's  $n$  (exponent on  $x$ ) seen in Figure 1(a) is not. This suggests that a sensible way to progress is to allow  $n$  to vary with tests conditions in the OSD model—i.e., to generalize the OSD model. But should this be with respect to stress or temperature? Because decreasing stresses are associated with increasing temperatures in Figure 1(a), it is not clear whether the observed fall in the value of  $n$  seen in Figure 1(a) is the result of a fall in stress or a rise in temperature. In the absence of any additional information, it is decided that the intercept of the isothermal lines be made temperature dependent, as in the original OSD model, but instead of treating the slope as a constant, it is made dependent on stress. Call this the generalized OSD model (GOSD).

### B. Functional Coefficients Representation of the Generalized OSD Model

A functional coefficients model starts with a specification of the relationships between a dependent variable and one or more explanatory variable. It then introduces other explanatory variables by using these additional variables to explain how the parameters of that relationship change. The functional coefficients representation of the GOSD parametric creep model starts with the isothermal representation in the OSD model

$$\ln(t_F) = a + b \ln(\sigma), \quad [3]$$

where  $b < 0$  (and  $b = -n$ ). Then, parameter  $a$  is made a function of temperature  $a = f(1/RT)$  and  $b$  a function of stress  $b = g(\ln(\sigma))$ . Other specifications are possible and lead to other well-known creep models. The difference between these well-known models and the functional coefficients model is that the functions  $f()$  and  $g()$  are left unspecified. Instead, they are approximated using a Taylor series. If this variation is modeled using a 1st order Taylor series expansion, then

$$a = a_0 + a_1 \left[ \left( \frac{1}{RT} \right) - \left( \frac{1}{RT_0} \right) \right], \quad [4a]$$

$$b = b_0 + b_1 (\ln(\sigma) - \ln(\sigma_0)), \quad [4b]$$

where  $b_0 = g(\ln(\sigma_0))$ ,  $a_0 = f(1/RT_0)$ ,  $b_1 = dg(\ln(\sigma_0))/d\ln(\sigma_0)$ ,  $a_1 = df(1/RT_0)/d\left(\frac{1}{RT_0}\right)$ —i.e., each derivative is evaluated at specific values for stress and temperature,

$\sigma = \sigma_0$  and  $T = T_0$ . This approximation can be done for all values of stress and temperature in a test matrix and so there are values for  $b_0$ ,  $b_1$ ,  $a_0$ , and  $a_1$  at each test condition making up the creep data set.

If a second-order Taylor series expansion is used to approximate  $g(\ln(\sigma))$  and  $f(1/RT)$ , then Eqs. [4] become

$$b = b_0 + b_1 (\ln(\sigma) - \ln(\sigma_0)) + b_2 (\ln(\sigma) - \ln(\sigma_0))^2, \quad [5a]$$

$$a = a_0 + a_1 \left[ \left( \frac{1}{RT} \right) - \left( \frac{1}{RT_0} \right) \right] + a_2 \left[ \left( \frac{1}{RT} \right) - \left( \frac{1}{RT_0} \right) \right]^2, \quad [5b]$$

where now  $b_0 = g(\ln(\sigma_0))$ ,  $a_0 = f(1/RT_0)$ ,  $b_1 = dg(\ln(\sigma_0))/d\ln(\sigma_0)$ ,  $a_1 = df(1/RT_0)/d\left(\frac{1}{RT_0}\right)$ ,  $b_2 = 0.5d^2g(\ln(\sigma_0))/d\ln(\sigma_0)^2$ ,  $a_2 = 0.5d^2f(1/RT_0)/d\left(\frac{1}{RT_0}\right)^2$ —with each derivative evaluated at  $\sigma = \sigma_0$  and  $T = T_0$ . So, the first model to be used in this paper will be termed a first-order functional coefficient version of the generalized OSD model (or GOSD1 for short) and the second model used in this paper is the second-order functional coefficient version of the generalized OSD model (or GOSD2 for short).

### C. Estimating the Functional Coefficients

The technique of least squares can be used to estimate values for all the above-mentioned derivatives by including a random error term  $\varepsilon$  to pick up the stochastic nature of creep failure times. Then inserting Eqs. [4] into Eq. [3] gives the single equation representation of the GOSD1 model

$$\ln(t_F) = \left[ a_0 - a_1 \frac{1}{RT_0} \right] + [b_0 - b_1 \ln(\sigma_0)] \ln(\sigma) + a_1 \frac{1}{RT} + b_1 [\ln(\sigma)]^2 + \varepsilon \quad [6a]$$

Values for  $a_1$ ,  $b_1$ ,  $[a_0 - a_1 \frac{1}{RT_0}]$ , and  $[b_0 - b_1 \ln(\sigma_0)]$  are then chosen to minimize  $\sum \varepsilon^2$ , where the sum is over all test conditions, of which there are say  $N$ , in the test matrix. Such a minimization has a well-known solution. This least square procedure therefore yields direct estimates for  $a_1$  and  $b_1$ . Parameters  $a_0$  and  $b_0$  are obtained indirectly by substituting in each existing stress-temperature test combination for  $\sigma_0$  and  $T_0$  in Eq. [6a]. For example, the least squares procedure will yield a value for  $[a_0 - a_1 \frac{1}{RT_0}]$  and  $a_1$ . If the least squares estimate for  $[a_0 - a_1 \frac{1}{RT_0}]$  is say  $\theta$ , then the value for  $a_0$  at a temperature of 823 K would be given by  $a_0 = \theta + a_1 \frac{1}{(8.314)823}$ .

Inserting Eqs. [5] into Eq. [3] gives the single equation representation of the GOSD2 model

$$\begin{aligned} \ln(t_F) = & \left[ a_0 - a_1 \frac{1}{RT_o} - a_2 \left( \frac{1}{RT_o} \right)^2 \right] \\ & + \left[ b_0 - b_1 \ln(\sigma_o) + b_2 (\ln(\sigma))^2 \right] \ln(\sigma) \\ & + \left[ a_1 - 2a_2 \frac{1}{RT_o} \right] \frac{1}{RT} + [b_1 - 2b_2 \ln(\sigma_o)] [\ln(\sigma)]^2 \\ & + a_2 \left( \frac{1}{RT} \right)^2 + b_2 [\ln(\sigma)]^3 + \varepsilon \end{aligned} \quad [6b]$$

So at each test condition  $a_2, b_2$  are estimated directly and the others indirectly. Higher order approximations can also be used. As Taylor series approximations are more accurate the closer the test condition is to  $(T_o, \sigma_o)$ , an additional way of improving the predictive accuracy is to accept that any specified functional coefficients model is only a realistic descriptor of creep over a restricted range of test conditions, for example, over conditions where the creep mechanism remains unchanged around  $(T_o, \sigma_o)$ . This can be achieved using the technique of weighted least squares. As stress and temperature are measured in different units, they must first be standardized using their means and standard deviations

$$\begin{aligned} x_1 = & [\ln(\sigma) \\ & - \text{mean of } \ln(\sigma)] / \text{standard deviation of } \ln(\sigma). \end{aligned} \quad [7a]$$

$$\begin{aligned} x_2 = & [1/RT \\ & - \text{mean of } 1/RT] / \text{standard deviation of } 1/RT. \end{aligned} \quad [7b]$$

The closeness of each test condition to test condition  $(T_o, \sigma_o)$  can then be measured as

$$d = |x_1 - x_{1,o}| + |x_2 - x_{2,o}|, \quad [7c]$$

where  $x_{1,o}$  is the standardized value for  $\ln(\sigma_o)$  and  $x_{2,o}$  is the standardized value for  $1/RT_o$ . Other distance measures, such as the Euclidean distance, can also be used, but using absolute values is more likely to make the distance measure robust to the presence of any unusually small or large failure times, i.e., to any outlying data points. Kernels can be used to determine the values for the weights,  $w$ . There are many such kernels in common use, but the one used by Cleveland<sup>[14]</sup> for LOESS procedures is the tri-cubic Kernel

$$w^2 = K_h(d/h) = \begin{cases} 0.864 \left( 1 - \left( \frac{d}{h} \right)^3 \right)^3 & \text{when } \left| \frac{d}{h} \right| < 1, \\ 0 & \text{otherwise} \end{cases}, \quad [7d]$$

and where  $h$  is a selected band width in the same “units” as  $d$ . While other kernels can be used (the Epanechnikov Kernel is also popular), the different Kernels tend to give similar weight values, but some Kernels may give

better lifetime predictions than others. This could form a possible topic for future research but is not the main scope of this paper. This paper uses the tri-cubic Kernel to enable broad comparisons to the results of Evans<sup>[9]</sup> that were obtained using this Kernel within his LOESS model.

For a selected target test condition  $(T_o, \sigma_o)$ ,  $w \ln(t_F)$  is regressed on the variables  $w, \ln(\sigma)w, (\ln(\sigma))^2 w$ , and  $w/RT$  (by minimizing  $\Sigma e^2$  in Eq. [8a])

$$\begin{aligned} w \ln(t_F) = & \left[ a_0 - a_1 \frac{1}{RT_o} \right] w + [b_0 - b_1 \ln(\sigma_o)] \ln(\sigma) w \\ & + a_1 \frac{w}{RT} + b_1 w [\ln(\sigma)]^2 + e \end{aligned} \quad [8a]$$

when using the GOSD1 model. Note that these weighted least squares estimates of  $a_1$  and  $b_1$  provide values for the required derivatives around the target test condition. When using GOSD2 model, the parameters in Eq. [8b] are chosen to minimize  $\Sigma e^2$

$$\begin{aligned} w \ln(t_F) = & \left[ a_0 - a_1 \frac{1}{RT_o} - a_2 \left( \frac{1}{RT_o} \right)^2 \right] \\ & + [b_0 - b_1 \ln(\sigma_o) + b_2 (\ln(\sigma))^2] \ln(\sigma) w \\ & + \left[ a_1 - 2a_2 \frac{1}{RT_o} \right] \frac{w}{RT} + [b_1 - 2b_2 \ln(\sigma_o)] w (\ln(\sigma))^2, \\ & + a_2 w \left( \frac{1}{RT} \right)^2 + b_2 w (\ln(\sigma))^3 + e \end{aligned} \quad [8b]$$

where  $e$  is a random disturbance term. A prediction of the time to failure at test condition  $(T_o, \sigma_o)$  is then given by Eq. [3] or equivalently Eqs. [8]. So, a weighted regression (often termed a local regressions) defined by Eqs. [8] is carried out for each test condition in the test matrix to yield an estimate for  $b_o, b_1, a_o, a_1$  (and  $a_2, b_2$  if using the GOSD2 model) at all such conditions. Notice that the weighted least squares procedure also depends on the bandwidth  $h$  that now needs further explanation.

#### D. Determining the Band Width, $h$

The band width  $h$  is on the same scale as  $d$  and so must be a value between the largest and smallest observed value for  $d$ . If  $h$  is set too large, the resulting creep predictions will be over generalizations leading to a poor prediction for any individual failure time. On the other hand, if  $h$  is set to low, the predictions may be so specific to the sample of failure times in the local regression that any extrapolation to other failure times may be unreliable—over fitting to the specific sample of data. As the value of  $d$  will depend on the test condition  $(T_o, \sigma_o)$ , it follows that the number of data points in each local regression will also be different. One approach to preventing over fitting is to use a “leave one data point out cross validation” procedure (see for example Fan *et al.*).<sup>[15]</sup> In this approach, Eq. [8a], when using the GOSD1 model, is replaced with

$$w \ln(t_F) = \left[ a_0 - a_1 \frac{1}{RT_o} \right] w + [b_0 - b_1 \ln(\sigma)] \ln(\sigma) w + a_1 \frac{w}{RT} + b_1 w (\ln(\sigma))^2 + \lambda D + e, \quad [9a]$$

where  $D$  is a dummy variable that equals 1 when  $(T, \sigma) = (T_o, \sigma_o)$  and zero otherwise. The parameter  $\lambda$  then measures the error made in predicting that value for  $\ln(t_F)$  at test condition  $(T_o, \sigma_o)$ , when this failure time recorded at  $(T_o, \sigma_o)$  is not used in the estimation of the other parameters in Eq. [9a]. Such a value for  $\lambda$  can be computed for all test conditions, then squared, and finally summed to obtain the sum of squared cross validation errors (SSCV)

$$SSCV = \sum_{i=1}^N \lambda_i^2, \quad [9b]$$

The band width  $h$  is then taken to be that value which minimize SSCV. The variable  $D$  can also be added to Eq. [8b] when using the GOSD2 model

$$w \ln(t_F) = \left[ a_0 - a_1 \frac{1}{RT_o} - a_2 \left( \frac{1}{RT_o} \right)^2 \right] w + [b_0 - b_1 \ln(\sigma_o) + b_2 (\ln(\sigma))^2] \ln(\sigma) w + \left[ a_1 - 2a_2 \frac{1}{RT_o} \right] \frac{w}{RT} + [b_1 - 2b_2 \ln(\sigma_o)] w (\ln(\sigma))^2 + a_2 w \left( \frac{1}{RT} \right)^2 + b_2 w (\ln(\sigma))^3 + \lambda D + e, \quad [9c]$$

#### IV. RESULTS

One of the aims of this paper is to use the functional coefficients representation of a generalized OSD model to predict failure times beyond an accelerated test data set. To do this, the accelerated creep data set is defined as all those test conditions in Figure 2 that have a failure time of 10,000 h or less. This accelerated data set is thus made up of  $N = 33$  failure times. The band width  $h$  is then calculated using just this accelerated test data set, using Eq. [9] to measure the value for  $\lambda_i$  at each of these  $i = 1$  to 33 test conditions (some repeated). Then suppose a prediction at test condition  $(T_o, \sigma_o)$  is required. If  $(T_o, \sigma_o) = (873 \text{ K}, 29 \text{ MPa})$ , this prediction would be an example of an extrapolation, while if  $(T_o, \sigma_o) = (873 \text{ K}, 115 \text{ MPa})$ , this prediction would be an example of an interpolation.

##### A. The Fully Parametric OSD Model

Applying least squares to Eq. [1b] using all 33 test results in the accelerated set of test data yielded the following result

$$\ln(t_F) = -1.179 - 5.063 \ln(\sigma) + 279.416 \left( \frac{1000}{RT} \right), \quad [10]$$

implying a Norton  $n$  value of 5.063 and an activation energy of  $279 \text{ kJ mol}^{-1}$ . However, the  $R^2$  value of 78.23 pct suggests a very poor fit to the short-term data shown as closed circles in Figure 3. The vertical axis of Figure 3 is the temperature-adjusted failure time given by  $\ln(t_F) - 279.416 \left( \frac{1000}{RT} \right)$ . Estimating the parameters of this fully parametric OSD model in this way results in predictions that have substantial systematic errors associated with them—both when predicting the short-term and long-term data. At moderate stresses, the predictions shown by the fitted line substantially underestimate the time to failure, but as stress falls toward values associated with typical operating conditions for this material, the model dramatically overestimates the time to failure. Unsurprisingly then, the model produces predictions for the longer-term data with an average absolute error of some 150 pct. These results can be used as a benchmark for comparisons with the GOSD1 and GOSD2 models.

##### B. A First-Order Functional Coefficients GOSD1 Model

Now consider the functional coefficients GOSD1 model that uses a 1st order Taylor series expansion to approximate coefficients  $a$  and  $b$  in Eq. [3]. The optimal band width estimated only from the accelerated tests data was found to be 2.2 using cross validation with  $SSCV = 0.00231$ . Figure 4 shows the estimates made for the parameters  $a_0, b_0, a_1,$  and  $b_1$  of this model at each of the 33 test conditions in the accelerated test data. The arrows highlight the parameter values obtained at test condition  $(T_o, \sigma_o) = (823 \text{ K}, 196 \text{ MPa})$ .

Before discussing the trends seen in Figure 4, it is informative to explain how these highlighted values were obtained. There were 22 such data points out of the 33 in the accelerated test matrix that had a  $K_h(d/h)$  value of less than 1 using  $h = 2.2$ . Figure 5 shows these 22 test conditions and the actual temperature-adjusted failure times associated with these conditions. These were calculated using an activation energy of creep of  $375 \text{ kJ mol}^{-1} - \ln(t_F) - 375 \left( \frac{1000}{RT} \right)$ . This value for the activation energy was obtained by minimizing  $\Sigma e^2$  in Eq. [8a] using just the 22 data points shown in Figure 5. The procedure yielded  $a_1 = Q_c = 374.876 \text{ kJ mol}^{-1}$ ,  $b_1 = 1.448$ ,  $[b_0 - b_1 \ln(\sigma_o)] = -22.808$ , and  $[a_0 - a_1 \frac{1}{RT_o}] = 37.337$ . These values for the parameters in Eq. [8a] define the dashed curve in Figure 5—which is the weighted regression curve. The arrow in Figure 4(b) shows this value for  $Q_c$ . Consequently, values for  $a_o$  and  $b_o$  can be derived from these estimates:  $b_o = -22.808 + 1.448 \ln(196) = -15.1634$  and  $a_o = 37.337 + 375.876 / (8.314 \times 723) = 92.124$ . The arrows in Figures 6(c) and (d) show these values for  $a_o$  and  $b_o$ . When  $\sigma = \sigma_o = 196 \text{ MPa}$ , Eq. [6a] collapses to

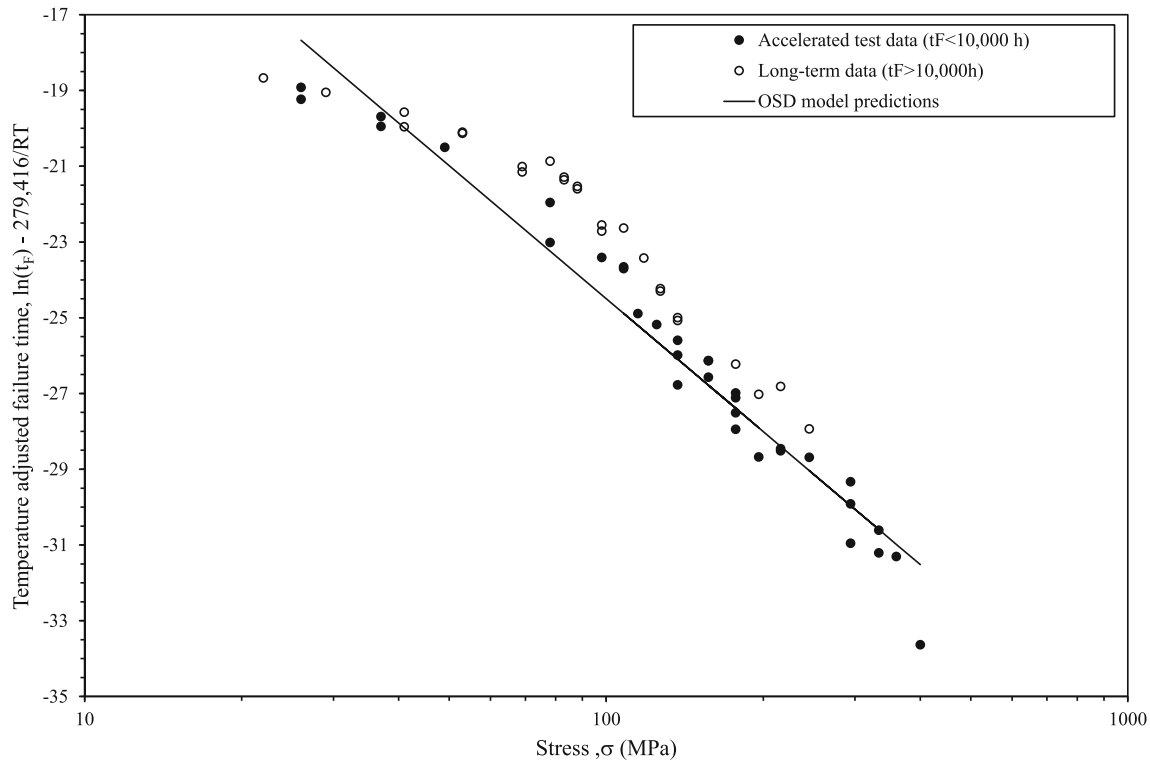


Fig. 3—Relationship between temperature compensated time to failure and stress using an activation energy estimated using least squares applied to the fully parametric OSD model.

$$\begin{aligned} \ln(t_F) &= a_0 - b_0 \ln(196) = 92.124 - 15.1635 \ln(196) \\ &= 12.09, \end{aligned} \quad [11]$$

which defines the arrow highlighted point of the dashed regression curve in Figure 5. This is an example of an interpolated failure time. This interpolation has a prediction error of some 7.28 pct. The above steps are repeated for each test condition, so that a separate weighted regression is computed yielding values for  $a_0$ ,  $b_0$ ,  $a_1$ , and  $b_1$  and an interpolated  $t_F$  value for all test conditions in the accelerated test data. The resulting parameter estimates are shown in Figure 4.

Clearly, higher order approximations will give better fits to the local data, but may not necessarily give a better failure time prediction. It does so at the test condition shown in Figure 5 because the point it is trying to predict is within the range of the accelerated data points used for the local fit. In some instances, especially in extrapolation, this may not be the case, and this is more likely the higher the order of approximation used (due to the skipping rope effect of using polynomials). So a balance needs to be struck between parsimony and accuracy of prediction.

Figure 4(a) shows the variation in Norton's  $n$  with test conditions, where  $n$  is the predicted change in  $\ln(t_F)$  following a small change in  $\ln(\sigma)$ , which from Eq. [6a] is found from the functional coefficients as  $[b_0 - b_1 \ln(\sigma_0)] + 2b_1 \ln(\sigma)$ . Figure 4(b) shows the variation in the activation energy for creep with test conditions. These two together are suggestive of specific changes in

creep mechanism with test conditions. The high values for  $n$  (ignoring the sign) and  $Q_c$  at the highest stresses indicate creep takes place through the generation and movement of new dislocations, formed at appropriate sources, since the yield stress of the material is exceeded. These new dislocations that are continuously generated due to the high stress leads to large net movement of atoms, and so contributes to high creep rates making failure times very sensitive to changes in stress (hence the very negative  $n$  values). This creep occurs largely because of these dislocations moving within the grains and under these circumstances  $Q_c$  is expected to be high and equivalent to that for self-diffusion in bainitic matrices. Figure 4(b) suggests this activation energy is  $Q_c \cong 420 \text{ kJ mol}^{-1}$ . Notice this value is much higher than the constant value of  $279 \text{ kJ mol}^{-1}$  obtained from the fully parametric OSD model.

At intermediate stresses, where the stress is below the yield stress, creep takes place within the grain boundary zones rather than in the grains, and this reflects itself in a lower activation energy for creep— $Q_c \cong 370 \text{ kJ mol}^{-1}$  in Figure 4(b)—representing diffusion along dislocations and grain boundaries. With fewer atoms moving the creep rate slows down and this reflects itself in a reduction in  $n$  to around  $-8$  in Figure 4(a). The change in  $n$  from around  $-18$  to  $-8$  (and  $Q_c$  from  $420$  to  $370 \text{ kJ mol}^{-1}$ ) then reflects the growing dominance of grain boundary creep as the stress falls. At the lowest stress, the activation energy increases again to approximately  $420 \text{ kJ mol}^{-1}$  in Figure 4(a). Wilshire and Whittaker [16] attributed this to the bainitic regions transforming to ferrite and coarse molybdenum carbide



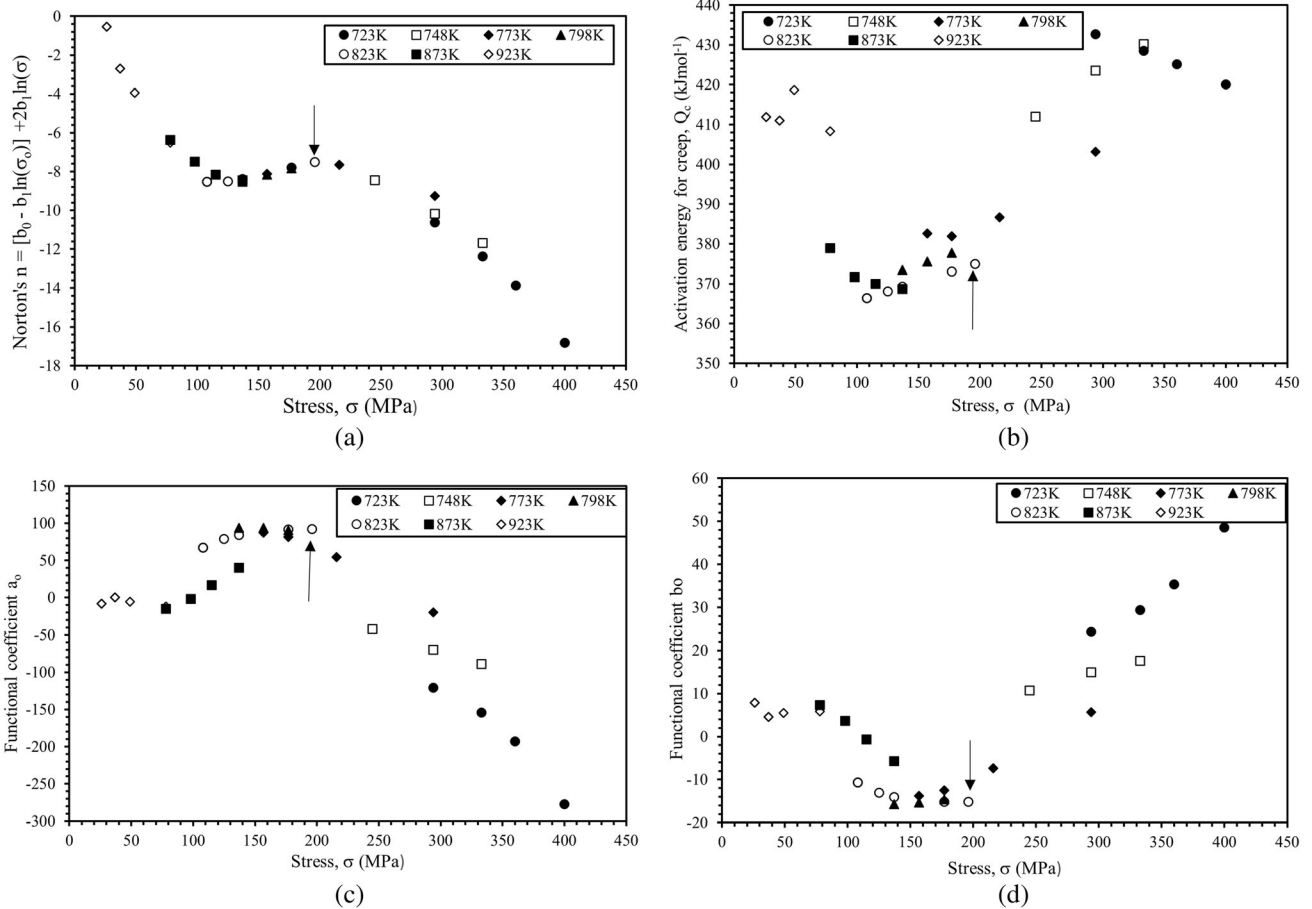


Fig. 4—Variations in (a) Norton's  $n$ , (b) the activation energy for creep, and (c, d) the structural coefficients  $a_0$  and  $b_0$ , with stress and temperature based on the GOSDI model.

particles in long-term tests at 923 K and very low stresses. This they argued would result in creep once again taking place within the grains where the activation energy is higher. But this is inconsistent with the continual reduction in the value of  $n$  seen in Figure 4(a)—the expectation would be for  $n$  to creep back to the values seen at the higher stresses if there was microstructural degradation. Instead, there is a tendency for  $n$  to diminish to a value of 1 at the very lowest stress and the highest temperature—and such conditions are usually associated with Nabarro-Herring diffusional creep. Such creep also leads to an  $n$  value of around 1 and an activation energy equal to that for self-diffusion as diffusion of atoms takes place only within the crystal lattice during Nabarro-Herring creep. This is consistent with the values seen in Figures 4(a) and (b) where  $n$  tends to 1 with decreasing stress and  $Q_c$  back to a value approaching  $420 \text{ kJ mol}^{-1}$ —that was taken above to be that associated with self-diffusion. Figures 4(c) and (d) shows the variation in the structural coefficients  $a_0$  and  $b_0$  with test conditions. Their changing values also reflect the above-mentioned changes in creep mechanism. While  $n$ ,  $a_0$ , and  $b_0$  show very little dependency on

temperature,  $Q_c$  appears to also show some temperature dependency.

The same procedure as above is used to make extrapolative predictions into the longer-term data—local weighted regressions were carried out using accelerated test conditions closest to the test conditions in the longer-term data set. For example, to get a prediction for the time to failure of a specimen tested at 216 MPa and 723 K, 19 data points out of the 33 in the accelerated test matrix had a  $K_h(\text{d/h})$  less than 1 using  $h = 2.2$ . A weighted regression through these 19 data points is used to predict the failure time at 216 MPa and 723 K following the same steps as demonstrated above for an interpolative prediction. Repeating this for all test conditions in the longer-term data sets produced the predictions shown in Figure 6, where they are plotted against the actual failure times beyond 10,000 h. The trend line through all the data points is quite close to the 1:1 line, and these predictions have an average absolute error  $|U|$  associated with them of 31.81 pct—which is a massive improvement on the error associated with the fully parametric OSD model of the previous subsection. The predictions are differing from this 1:1 line for three reasons. The first is because the slope of the

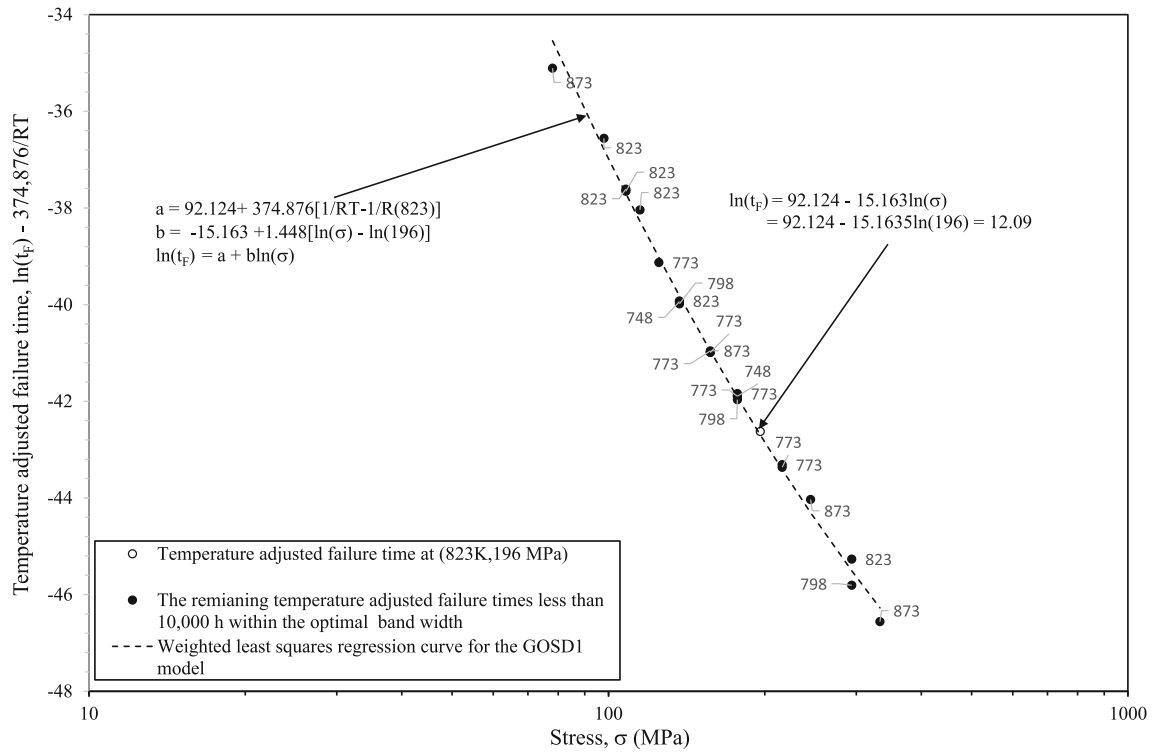


Fig. 5—Local test conditions used to interpolate the failure time at 196 MPa and 823 K, together with the weighted regression curve through the nearest 22 data points to this test condition.

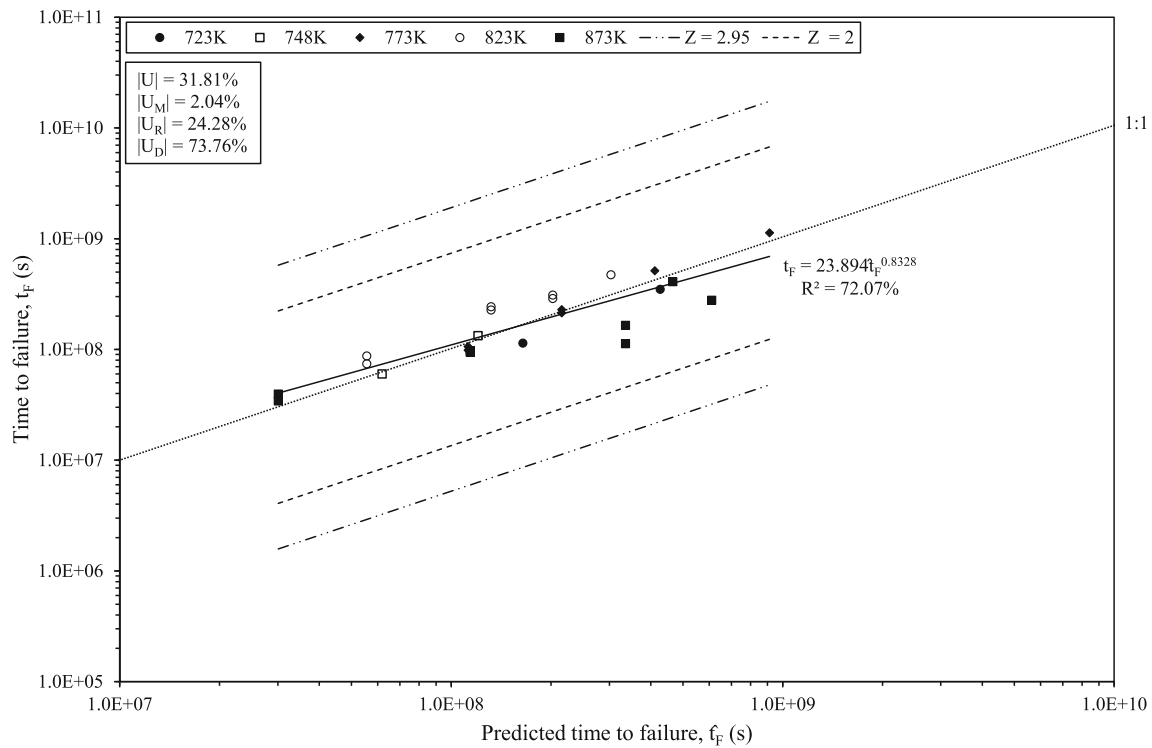


Fig. 6—Plot of actual against predicted failure times beyond 10,000 h using the GOSD1 model. The U statistics are as calculated by Evans.<sup>[17]</sup>

best fit line of 0.83 differs from 1 and this accounts for some 24.28 pct of  $|U|$  (as revealed by  $|U_R|$ —see Evans<sup>[17]</sup> for details on how to calculate these  $U$  values). Secondly, the average of the predictions differs from the average of the actual failure times by 0.0095 and this accounts for some 2.04 pct of  $|U|$  (as revealed by  $|U_M|$ ). In part this reflects itself in the intercept of the trend line in Figure 6 (23.894) differing from zero. The rest of the error is random in nature, and this accounts for some 73.76 pct of  $|U|$  (as revealed by  $|U_D|$  and the  $R^2$  value of less than 100 pct). Figure 6 also reveals that most of the prediction errors occur at the lowest stresses at temperature of 873 K. The  $Z$  value shown in Figure 6 is given by  $Z = e^{2.58s_e}$ , where  $s_e$  is the standard deviation in the percentage prediction errors. Ideally, for single-cast assessment,  $Z$  should be less than or equal to 2, whereas  $Z \geq 4$  is unacceptable according to Holdsworth *et al.*<sup>[18,19]</sup> While this value is slightly above 2, its value is acceptable according to Holdsworth and substantially below the  $Z$  value for the fully parametric OSD model where  $Z = 13.18$ .

Evans<sup>[9]</sup> found that for the LOESS version of the OSD model, the average absolute error  $|U|$  was 55.68 pct and 46.84 pct of this error was random in nature. On both measures, the LOESS model produces inferior extrapolations.

### C. A Second-Order Functional Coefficients GOSD Model

Figure 7 shows the variation of the GOSD2 model parameters with stress and temperature estimated using just the accelerated test data. Figure 7(a) shows the variation in Norton's  $n$  with test conditions, where  $n$  is the predicted change in  $\ln(t_F)$  following a small change in  $\ln(\sigma)$ , which from Eq. [6b] is found from the functional coefficients as  $[b_0 - b_1 \ln(\sigma_0) + b_2 \{\ln(\sigma_0)\}^2] + [b_1 - 2b_2 \ln(\sigma_0)] + 3b_2 \ln(\sigma_0)$ . Figure 7(b) shows the variation in the activation energy for creep with test conditions. The trends with respect to stress seen in these two figures are broadly consistent with those obtained using the first-order approximation

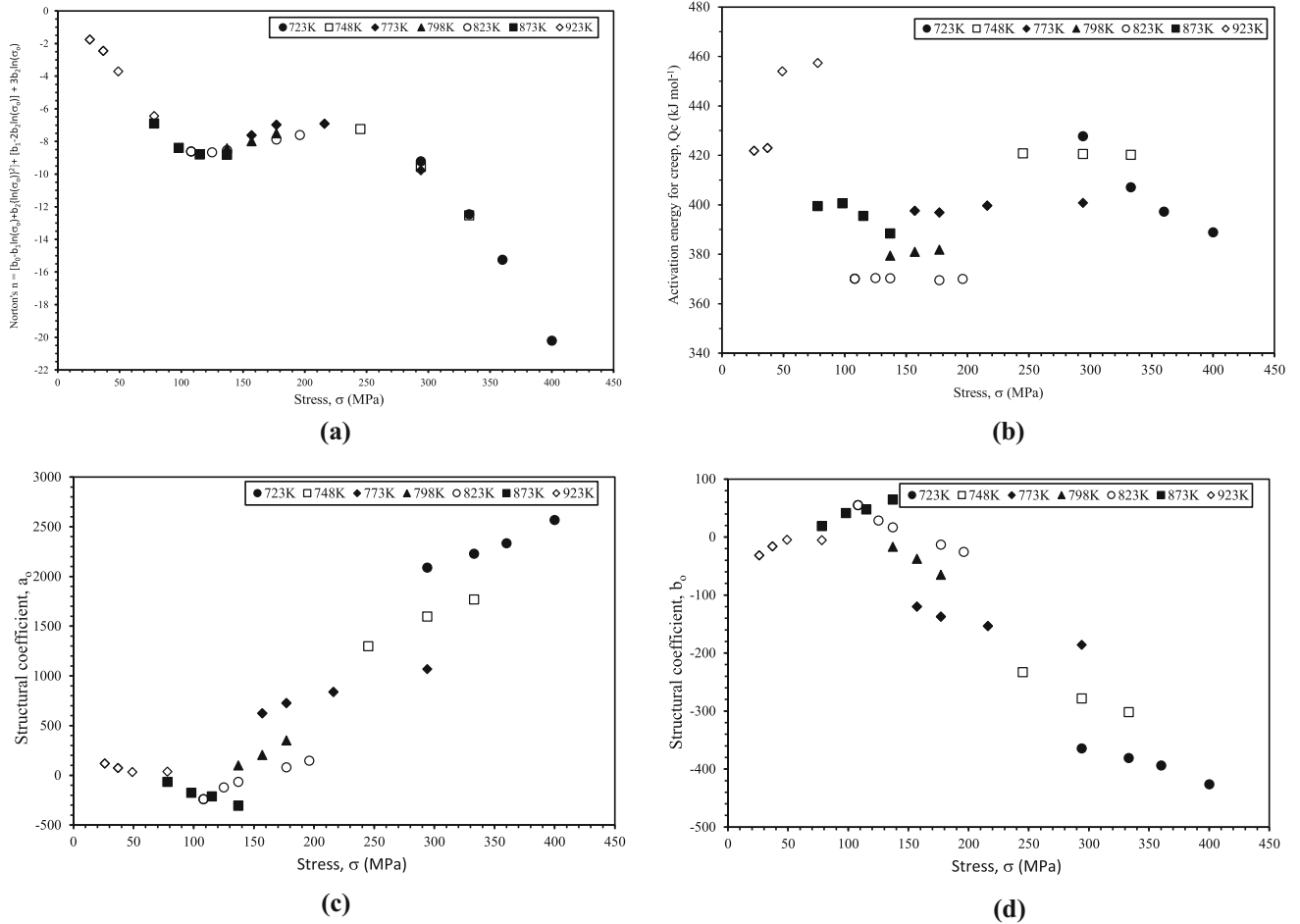


Fig. 7—Variations in (a) Norton's  $n$ , (b) the activation energy for creep, and (c–d) the structural coefficients  $a$  and  $b$ , with stress and temperature using the GOSD2 model.

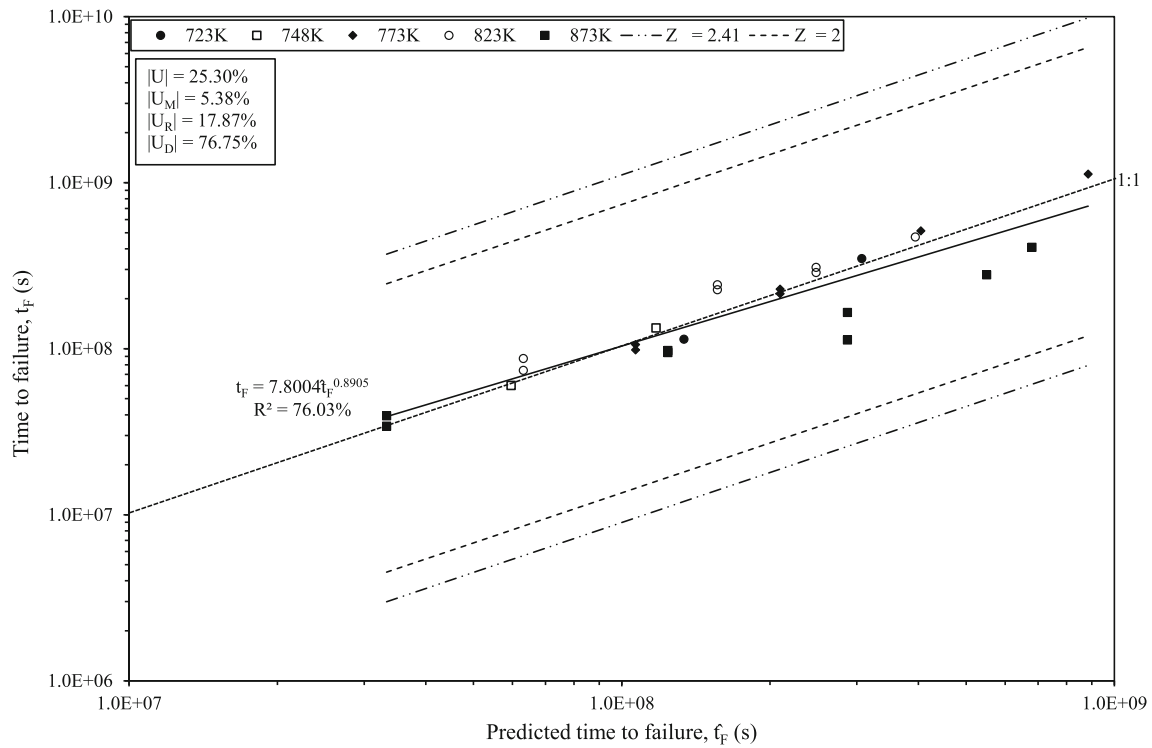


Fig. 8—Plot of actual against predicted failure times beyond 10,000 h using the GOSD2 model. The U statistics are as calculated by Evans.<sup>[17]</sup>

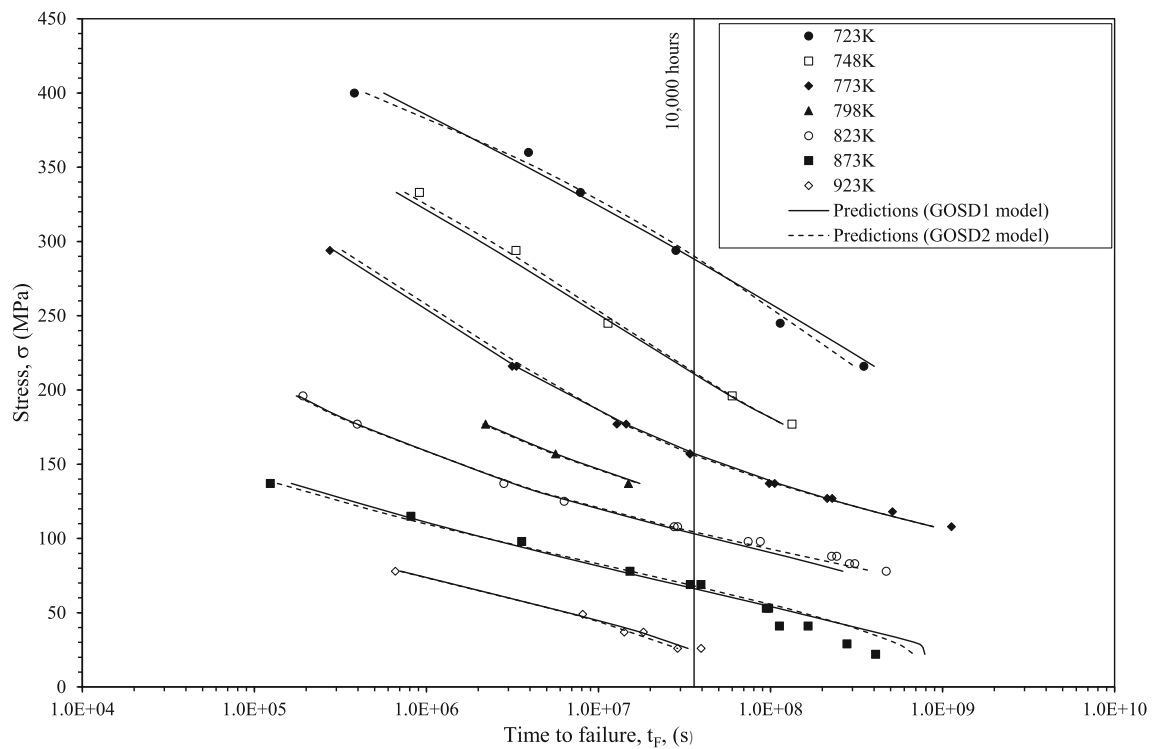


Fig. 9—Plot of time to failure against stress together with the predictions from the GOSD1 and GOSD2 models.

[Figures 4(a) and (b)] and so support the conclusions drawn in the previous sub section with regard to changing creep mechanisms.

The GOSD2 model was then used to extrapolate into the longer-term data. The results are shown in Figure 8

where these predictions are plotted against the actual failure times beyond 10,000 h. The trend line through all the data points is quite close to the 1:1 line, and these predictions have an average absolute error  $|U|$

associated with them of 25.3 pct which is some 6 percentage points lower compared to the GOSD1 model.

But again, the predictions are differing from this 1:1 line for three reasons. The first is because the slope of the best fit line of 0.89 differs from 1 and this accounts for some 17.87 pct of  $|U|$  (as revealed by  $|U_R|$ , and which is some 6 percentage points lower than when using the first-order approximation). Secondly, the average of the predictions differs from the average of the actual failure times by 0.022 and this accounts for some 5.38 pct of  $|U|$  (as revealed by  $|U_M|$ , which is about 3 percentage points higher than when using the first-order approximation). The rest of the error is random in nature, and this accounts for some 76.75 pct of  $|U|$  (as revealed by  $|U_M|$ , which is about 3 percentage points higher than when using the GOSD1 model). Figure 9 also reveals that most of the prediction errors occur at the lowest stresses at temperature of 873 K. In summary then, using the GOSD2 model over the GOSD1 model results in a set of predictions with a lower overall mean absolute percentage error, and with the proportion of this error that is random in nature being slightly higher—and so a slightly lower systematic error. The  $Z$  value for this model is also closer to 2 compared to the GOSD1, but like the first-order model most of the prediction errors are associated with a temperature of 873 K.

Finally, Figure 9 plots the long-term predictions from the first- and second-order functional coefficients version of the OSD model in the more familiar stress  $v$  failure time space. This reinforces the points made above where the predictions are good from both models at all temperature but 873 K. But at this temperature, the GOSD2 model performs best.

## V. CONCLUSION

This paper has demonstrated the inadequacy of using the fully parametric OSD creep model for predicting long-term failure times for 2.25Cr–1Mo from accelerated test data. This failure was explained by non-constant model parameters—the result of changing creep mechanisms. The paper then introduces a semi-parametric estimation procedure for a generalized OSD model (a structural coefficients version of the GOSD model) that can be used to deal with changing creep mechanisms while maintaining the structure of the parametric model and consequently produce more reliable long-term predictions compared to the fully parametric version. When this technique was applied to 2.25Cr–1Mo steel, it was found that the model parameters varied in line with changing creep mechanisms but in a partially different way compared to that already suggested in the literature for this material. With diminishing stress and increasing temperature, dislocation creep within the crystal structure morphs into grain boundary dislocation motion and finally Nabarro-Herring creep. The functional coefficients models produced better long-term extrapolations compared to both the fully parametric OSD model and the LOESS method

introduced by Evans. Areas for future work include applying this technique to other steels and high-temperature materials and extending the approach by specifying different forms for parameters  $a$  and  $b$ —perhaps by allowing  $a$  and  $b$  to vary with both stress and temperature.

## FUNDING

This research was not funded by research council grants or private sponsors and as such there are no financial relationships to declare.

## OPEN ACCESS

This article is licensed under a Creative Commons Attribution 4.0 International License, which permits use, sharing, adaptation, distribution and reproduction in any medium or format, as long as you give appropriate credit to the original author(s) and the source, provide a link to the Creative Commons licence, and indicate if changes were made. The images or other third party material in this article are included in the article's Creative Commons licence, unless indicated otherwise in a credit line to the material. If material is not included in the article's Creative Commons licence and your intended use is not permitted by statutory regulation or exceeds the permitted use, you will need to obtain permission directly from the copyright holder. To view a copy of this licence, visit <http://creativecommons.org/licenses/by/4.0/>.

## DATA AVAILABILITY

All data used in this publication are in the public domain: References 6, 7.

## COMPETING INTEREST

The authors report there are no competing interests to declare.

## REFERENCES

1. S. R. Holdsworth and G. Merckling: ECCC developments in the assessment of creep-rupture data. In: Proceedings of the Sixth International Charles Parsons Conference on Engineering Issues in Turbine Machinery, Power Plant and Renewables, Trinity College, Dublin, 16–18 September 2003.
2. F.R. Larson and J.A. Miller: *Trans. ASME*, 1952, vol. 174, p. 5.
3. S. S. Manson, and A. M. Haferd: A linear time-temperature relation for extrapolation of creep and stress-rupture data. NACA Technical Note 2890; National Advisory Committee for Aeronautics: Cleveland, 1953. *Materials* 2017, 10, 1190–29 of 30–15.
4. J. E. Dorn and L. A. Shepherd: What we need to know about creep. In: Proceedings of the STP 165 symposium on the effect of cyclical heating and stressing on metals at elevated temperatures, Chicago, 17 June 1954.
5. F.C. Monkman and N.J. Grant: *Proc. Am. Soc. Test. Mater.*, 1956, vol. 56, pp. 593–620.

6. IMS Creep Data Sheet No. 3B: Data Sheets on the Elevated-Temperature Properties of 2.25Cr-1Mo Steel for Boiler and Heat Exchanger Seamless Tubes (STBA 24), National Research Institute for Metals, Tokyo.
7. NIMS Creep Data Sheet No.50A: Long-Term Creep Rupture Data obtained after Publishing the Final Edition of the Creep Data Sheets, National Research Institute for Metals, Tokyo.
8. Y.P. Ding, X.J. Wu, R. Liu, X.Z. Zhang, and F. Khelifaoui: *Thermal Sci. Eng. Progress*, 2023, vol. 36, 101603.
9. M. Evans: *International Journal of pressure Vessels and Piping*, 2023, 206, Start page: 105047.
10. S.S. Manson, U. Muraldihan, Analysis of creep rupture data in five multi heat alloys by minimum commitment method using double heat term centring techniques, in: *Progress in Analysis of Fatigue and Stress Rupture MPC-23*, ASME, New York, 1983, pp. 1–46.
11. I.I. Trunin, N.G. Golobova, E.A. Loginov, New methods of extrapolation of creep test and long time strength results, In: *Proceedings of the 4th International Symposium on Heat Resistant Metallic Materials*, Mala Fatra, 1971.
12. Z. Cai, J. Fan, and Q. Yao: *J. Am. Stat. Assoc.*, 2000, vol. 95(451), pp. 941–56.
13. B. Wilshire and A.J. Battenbough: Creep and creep fracture of polycrystalline copper. *Mater. Sci. Eng. A*, 2007, vol. 443, pp. 156–66.
14. W.S. Cleveland: Robust locally weighted regression and smoothing scatterplots. *J. Am. Stat. Assoc.*, 1979, vol. 74, pp. 829–36.
15. J. Fan, I. Gijbels, T.-C. Hu, and L.-S. Huang: *Stat. Sin.*, 1996, vol. 6(1), pp. 113–27.
16. M. Whittaker and B. Wilshire: *Mater. Sci. Eng. A*, 2010, vol. 527(18–19), pp. 4932–938.
17. M. Evans: *Mater. High Temp.*, 2023, vol. 40(6), pp. 457–68.
18. S.R. Holdsworth, G. Merckling, ECCC developments in the assessment of creep-rupture data. In: *Proceedings of sixth international Charles Parsons Conference on engineering issues in turbine machinery, power plant and renewables*, Trinity College, Dublin, 16–18 September, 2003.
19. S.R. Holdsworth: Developments in the assessment of creep strain and ductility data. *Mater. High Temp.*, 2004, vol. 21(1), pp. 125–32.

**Publisher's Note** Springer Nature remains neutral with regard to jurisdictional claims in published maps and institutional affiliations.